DOI:10.22337/2587-9618-2025-21-4-73-82

AN EXPERIMENTAL INVESTIGATION OF THE THERMOMECHANICAL PERFORMANCE OF WOOD STRUCTURES ASSEMBLED WITH DENSIFIED WOODEN DOWELS UNDER FIRE EXPOSURE

***T.T. Tran* [1], *M. Khelifa* [2], *M. Oudjene* [3], *M. Debal* [2], *Y. Rogaume* [2]**

[1] Hanoi Architectural University, Hanoi, VIETNAM
[2] University of Lorraine, Epinal, FRANCE
[3] Department of Civil and Water Engineering, University of Laval, Québec, CANADA

Abstract: This study presents an experimental investigation into the thermomechanical behavior of wood structures assembled with densified wooden dowels under fire exposure. The research focuses on Adhesive-Free Engineered Wood Products (AFEWPs), particularly adhesive-free cross-laminated timber (AFCLT) panels, and timber connections incorporating either thermo-mechanically compressed wooden dowels or conventional steel dowels. A series of thermal and thermomechanical tests were conducted to evaluate internal temperature distribution, charring behavior, and structural displacement at elevated temperatures. The fire performance of dowel-type connections was assessed by comparing the thermal response and deformation of joints using wooden and steel dowels. The results indicate that timber connections incorporating densified wooden dowels exhibited better thermal insulation and lower charring rates compared to those with steel dowels, thereby improving the overall fire resistance of the jointed assemblies. This study highlights the potential of densified wood dowel as a sustainable and fire-resilient alternative to metallic fasteners in engineered wood. structures.

Keywords: Thermomechanical behavior, Densified wooden dowels, Adhesive-Free Engineered Wood Products (AFEWPs), Adhesive-Free Cross-Laminated Timber (AFCLT), Timber connection, Sustainable fasteners, Engineered wood structures

ЭКСПЕРИМЕНТАЛЬНОЕ ИССЛЕДОВАНИЕ ТЕРМОМЕХАНИЧЕСКИХ ХАРАКТЕРИСТИК ДЕРЕВЯННЫХ КОНСТРУКЦИЙ, СОБРАННЫХ С ПОМОЩЬЮ УПЛОТНЕННЫХ ДЕРЕВЯННЫХ НАГЕЛЕЙ, ПРИ ОГНЕВЫХ ВОЗДЕЙСТВИЯХ

***Т.Т. Тран* [1], *М. Хелифа* [2], *М. Уджене* [3], *М. Дебал* [2], *Ю. Рогаум* [2]**

[1] Ханойский архитектурный университет, г. Ханой, ВЬЕТНАМ
[2] Университет Лотарингии, ЛЕРМАБ, г. Эпинал, ФРАНЦИЯ
[3] Факультет гражданского и водного строительства, Университет Лаваля, г. Квебек, КАНАДА

Аннотация: В данном исследовании представлены результаты экспериментального изучения термомеханического поведения деревянных конструкций, соединенных с помощью уплотненных деревянных нагелей, при огневом воздействии. В исследовании рассматриваются безклеевые соединения деревянных элементов (AFEWP), в частности, панелей из перекрестно-ламинированной древесины (AFCLT) и деревянных соединений, в которых используются термомеханически спрессованные деревянные нагели или обычные стальные нагели. Была проведена серия термических и термомеханических испытаний для оценки внутреннего распределения температуры, поведения при обугливании и деформации конструкции при повышенных температурах. Пожаростойкость соединений с использованием нагелей оценивалась путем сравнения теплового сопротивления и деформации соединений с использованием деревянных и стальных нагелей. Результаты показывают, что деревянные соединения с использованием уплотненных деревянных нагелей демонстрировали лучшую теплоизоляцию и более низкие показатели обугливания по сравнению с соединениями со стальными нагелями. Это улучшало общую пожаростойкость соединенных конструкций. Данное исследование подчеркивает потенциал уплотненных деревянных нагелей как экологичной и огнестойкой альтернативы металлическим крепежным элементам в конструкциях из древесины.

Ключевые слова: термомеханическое поведение, уплотненные деревянные нагели, деревянные элементы с безклеевым соединением (AFEWP), поперечно-ламинированная древесина без клея (AFCLT), соединение элементов из древесины, экологичные крепежные элементы, конструкции из дерева

INTRODUCTION

The environmental impact of the construction industry is substantial, with buildings accounting for approximately 40% of global energy consumption and up to 33% of greenhouse gas (GHG) emissions worldwide. In response, recent initiatives have promoted the use of renewable and low-carbon materials, particularly engineered wood products (EWPs) such as glued laminated timber (glulam) and cross-laminated timber (CLT). These materials store carbon and are derived from renewable resources, making them attractive for sustainable construction. However, their widespread use is constrained by the reliance on petrochemical-based adhesives, which pose challenges in terms of recyclability, environmental compatibility, and long-term durability.

To address these limitations, the North-West-European Interreg research initiative "Towards Free Adhesive Buildings (AFTB)" has introduced a new class of Adhesive-Free Engineered Wood Products (AFEWPs), which utilize thermo-mechanically densified wood dowels as mechanical connectors in place of traditional adhesives. These dowels exhibit a shape-memory effect—commonly referred to as "strain recovery"—that allows them to swell in pre-drilled holes and form tight, durable joints under varying humidity conditions [1]. This connection concept not only eliminates synthetic adhesives but also supports the development of scalable, fully wooden structural systems aligned with sustainability goals.

While the mechanical performance of densified wood dowel joints has been studied to some extent [2-14], their behavior under elevated temperatures remains underexplored. Given the inherent combustibility of timber, understanding the thermal and thermomechanical response of these adhesive-free connections is essential for assessing their viability in fire-exposed environments. Recent research has begun addressing this gap through both experimental and numerical investigations [15], highlighting the need to evaluate fire-induced thermal degradation, heat transfer, and structural deformation in dowel-connected wood assemblies.

To further this understanding, the present study conducts an experimental program focusing on both adhesive-free cross-laminated timber (AFCLT) panels and dowel-type timber connections. The AFCLT panels were exposed to radiant heat fluxes of 49 and 60 kW/m², with the primary objective of assessing charring depth as an indicator of fire-induced degradation. These panel-scale tests are designed to complement prior cone calorimeter experiments conducted on natural and densified wood [15], providing additional insight into heat penetration and material loss under realistic fire exposure.

In parallel, timber connections assembled with either densified wooden dowels or conventional steel dowels were subjected to the same heat flux levels. For these connections, detailed measurements were performed to capture temperature profiles, char layer evolution, and thermally induced displacements. Instrumentation included embedded thermocouples and displacement sensors to monitor the coupled thermal–mechanical response of each joint configuration, while a 3D laser scanning technique was employed to quantify the charring profile on exposed surfaces. This two-part experimental approach enables direct comparison between panel-level and connection-level behavior, offering a comprehensive understanding of the influence of connector type on fire performance. Overall, the findings aim to validate the use of densified wood dowels as a viable, fire-resilient, and sustainable alternative to metallic fasteners in engineered wood structures.

EXPERIMENTAL SETUP

Fire testing of CLT panels asembled with densified wooden dowels

Fire resistance tests were conducted on adhesive-free cross-laminated timber (CLT) panels to evaluate the thermal performance of densified wooden dowels used as mechanical connectors. Each CLT specimen consisted of three orthogonally laminated layers, with each layer composed of three oak panels measuring 150 × 450 mm and 25 mm in thickness. The detailed panel dimensions are provided in Figure 1. The layers were connected using densified spruce dowels with a diameter of 16 mm. Both the oak panels and dowels had a uniform moisture content of 10%.

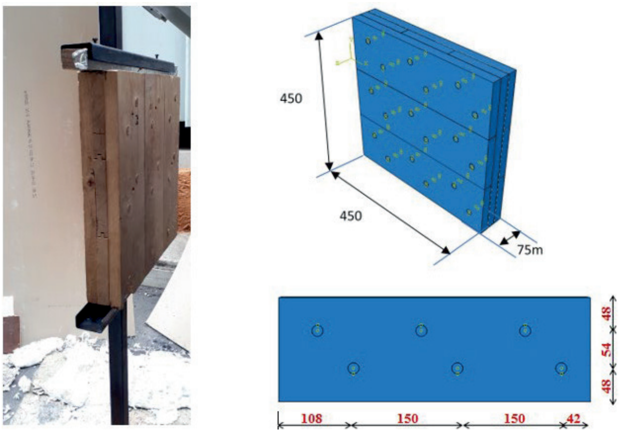

Figure 1. Adhesive-free CLT panel geometry and specimen dimensions

The experimental setup for the fire test of Adhesive-free CLT panels is illustrated in Figure 1. A dedicated test furnace was developed for this purpose, employing four radiant panels as the heat source. Each panel delivered a nominal heat flux of 100 kW/m² and could reach surface temperatures up to approximately 2000 °C. The CLT specimens were horizontally exposed to constant external heat fluxes. Depending on the desired intensity, the distance between the panels and the specimen surface was set at either 20 cm for 60 kW/m² or 30 cm for 49 kW/m². Two replicate tests were conducted for each heat flux level.

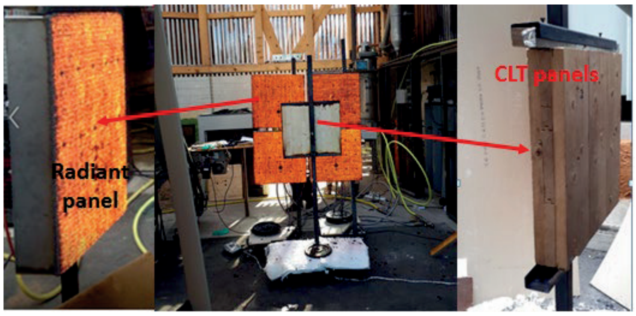

Figure 2. Testing diagram of fire test of Adhesive-free CLT panels

Thermo-mechanical testing of L-shaped connection assembled with densified wood dowels

To evaluate the structural performance of densified wooden dowels, fire tests were conducted on L-shaped timber connections composed of a column and a beam. Each specimen incorporated four dowels with a diameter of 16 mm, joining three-layer laminates with 32 mm thickness per layer. The CLT panels were made from the same material described previously. The experimental results were used to compare the performance of densified dowels with conventional steel dowels. Geometrical details of the connection and the finite element model are provided in Figure 3. Oak wood was used for the laminates in both tests, with an average measured moisture content of 10%. The fire tests were conducted for two types of dowel materials: conventional steel and densified spruce. This comparison enables an evaluation of the effectiveness of using compressed wooden dowels as an alternative to traditional steel connectors.

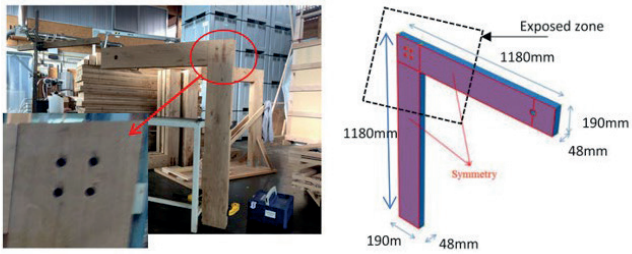

Figure 3. Detailed structure of L-shaped connection

Figure 4 illustrates the fire testing setup for L-shaped timber connections. Radiant panels, each rated at 100 kW/m² and capable of reaching 2000 °C, provided controlled heat exposure. To limit edge effects, gypsum plasterboards were used as thermal shields. Specimens were exposed horizontally to constant heat fluxes of 49 and 60 kW/m², achieved by adjusting the heater distance to 30 cm and 20 cm, respectively. The heating regime was calibrated to match the ISO 834 [16] standard, ensuring consistency with Eurocode 5 [17] assumptions.

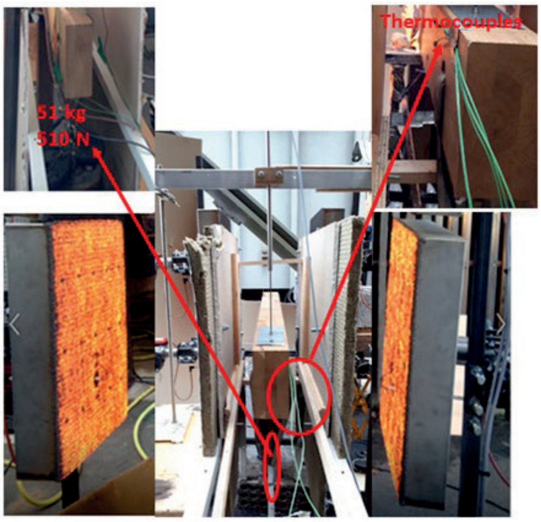

Figure 4. Experimental setup for thermo-mechanical testing of connections

Surface temperatures were monitored using a multispectral infrared camera, while internal temperatures were recorded every second via a USB TC-08 PICO system. Type K thermocouples (1 mm diameter) were embedded at multiple depths in both timber layers and dowels. Deflections were tracked using LVDTs at the free end of each specimen. Two repeated tests were conducted for each dowel type and heat flux condition.

RESULTS AND DISCUSSION

Time–temperature profiles in reinforced L-joints

Figures 5–8 present time–temperature profiles recorded in an L-joint specimen reinforced with either densified wooden dowels (Figs. 5 and 6) or steel dowels (Figs. 7 and 8) under radiant heat fluxes of 49 kW/m² and 60 kW/m². Each plot shows temperature traces at the joint surface (0 mm) and at increasing depths (2 mm, 3 mm, up to 6 mm), thereby capturing the thermal response of both the wood layer and the dowel material. By juxtaposing these data, one can directly assess how heat-flux intensity, dowel thermal conductivity, and sensor depth govern the rate of temperature rise, peak temperatures achieved, and overall thermal gradient across the connection. The following discussion elaborates on these interactions and their implications for fire performance.

Under a 60 kW/m² heat flux, the L-joint heats up significantly faster than under 49 kW/m². For example, the surface sensor (Test–0 mm) reaches 400 °C in about 350 s at 60 kW/m², compared to roughly 500 s at 49 kW/m². Likewise, the temperature difference between shallow and deeper sensors grows larger at the higher flux, indicating a steeper thermal gradient through the joint.

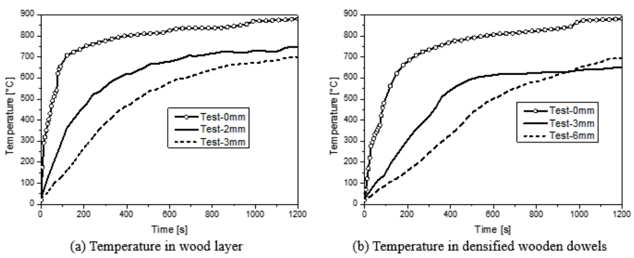

Figure 5. Temperature evolution in an L-joint reinforced with densified wooden dowels under a 49 kW/m² heat flux

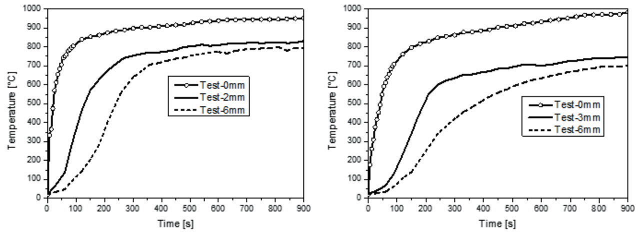

(a) Temperature in wood layer (b) Temperature in densified wooden dowels

Figure 6. Temperature evolution in an L-joint reinforced with densified wooden dowels under a 60 kW/m² heat flux

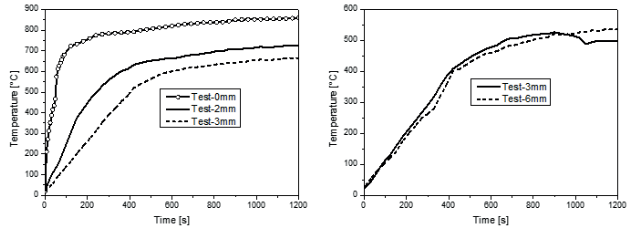

(a) Temperature in wood layer (b) Temperature in steel dowels

Figure 7. Temperature evolution in an L-joint reinforced with steel dowels under a 49 kW/m² heat flux

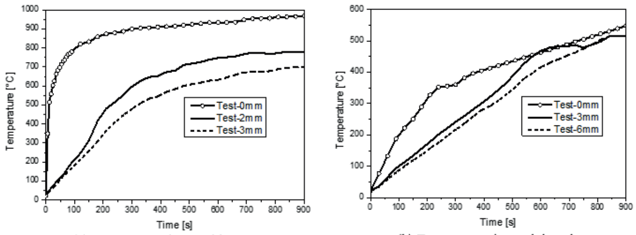

(a) Temperature in wood layer (b) Temperature in steel dowels

Figure 8. Temperature evolution in an L-joint reinforced with steel dowels under a 60 kW/m² heat flux

When reinforced with densified wooden dowels, the joint exhibits a much slower heat-up rate than with steel dowels. After 1 200 s at 49 kW/m², the wooden dowel surface remains below 700 °C, whereas with steel dowels it approaches 900 °C in only ~1 000 s. The low thermal conductivity of the wooden dowels provides additional insulation, while the high conductivity of steel creates a pronounced thermal bridge that accelerates heat transfer into the wood substrate.

Sensor depth further highlights these differences. In wooden-dowel joints, Test–2 mm and Test–3 mm lag the surface by 100–150 °C at equivalent times, demonstrating effective heat resistance. In contrast, steel-dowel joints show only a 20–30 s delay between the surface and a 6 mm depth, reflecting rapid conduction through the metal dowel even at greater depths.

Overall, densified wooden dowels markedly extend the time to critical temperatures and improve fire performance of L-joints, making them preferable where fire resistance is paramount. Steel dowels, while mechanically robust, accelerate heat ingress and risk earlier structural compromise. These effects intensify at higher heat fluxes. For fire-sensitive connections, designers should favor wooden dowels or incorporate thermal insulation when steel dowels are unavoidable.

Post-fire residual cross-section measurement

Figure 9 illustrates the laser-scanning arrangement used to capture the post-fire geometry of the CLT panel and L-joint specimens.

Figure 9. Laser-scanning setup for post-fire residual cross-section measurement

After carefully removing the charred surface layer, a high-resolution terrestrial laser scanner was mounted on a fixed tripod at a known distance and orientation relative to each joint. The scanner emitted a dense grid of laser pulses across the exposed cross-section, generating a 3D point cloud with sub-millimetre accuracy in less than two minutes per specimen. Custom software then interpolated these points to reconstruct the true residual timber profile, enabling precise measurement of section loss and deformation. Compared with conventional caliper or ruler methods, this non-contact approach greatly accelerates data collection, minimizes human error, and delivers a comprehensive, high-fidelity record of the remaining cross-section.

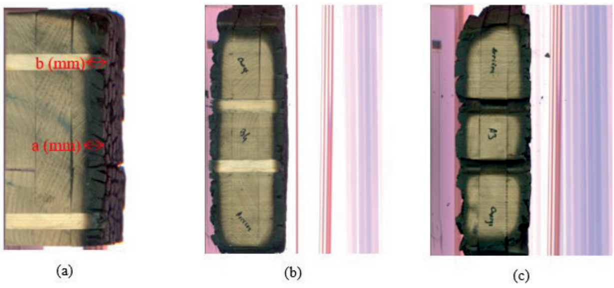

Figure 10. Residual cross-sections after fire exposure: (a) CLT panel; (b) L-joint reinforced with densified wooden dowels; (c) L-joint reinforced with steel dowels

Figure 10 displays the residual char across three specimens: in the unreinforced CLT panel (a), the char layer forms uniformly across the cross-section, indicating surface-controlled heat transfer; similarly, the L-joint reinforced with densified wooden dowels (b) maintains a generally even char depth, with only slight deepening adjacent to each dowel, demonstrating their insulating effect; by contrast, the steel-dowel joint (c) exhibits pronounced, irregular charring along and around each metal connector, evidencing thermal bridging that accelerates interior wood degradation.
Tables 1–3 summarize char depths measured in CLT panels and L-joints reinforced with densified wooden or steel dowels after exposures to 49 kW/m² or 60 kW/m² for 15 min or 20 min.

Table 1. Charring depth in CLT panels after fire exposure

Speciment	Heat flux (kW/m^2)	Time (min)	a (mm)	b (mm)
Panel 1	49	15	13	10,5
Panel 2	49	15	15	11
Panel 3	60	15	15	11,5

Table 2. Charring depth in L-joint reinforced with densified wooden dowels after fire exposure

Speciment	Heat flux (kW/m^2)	Time (min)	a (mm)	b (mm)
Connection 1	49	20	15	12
Connection 2	49	20	14,5	10
Connection 3	60	15	16	11
Connection 4	60	15	16.5	11

Table 3. Charring depth in L-joint reinforced with steel dowels after fire exposure

Speciment	Heat flux (kW/m^2)	Time (min)	a (mm)	b (mm)
Connection 1	49	20	17	-
Connection 3	60	15	17	-
Connection 4	60	15	17	-

Quantitatively, CLT panels exhibited a = 13 mm and b = 10.5 mm at 49 kW/m² for 15 min, and a = 15 mm and b = 11.5 mm at 60 kW/m² for 15 min. In comparison, wooden-dowel L-joints showed slightly greater surface char, a = 14.5 mm (Δ +1.5 mm) and b = 10 mm (Δ –0.5 mm) at 49 kW/m²/15 min, and increased further to a = 15 mm and b = 12 mm at 49 kW/m²/20 min, indicating that longer exposure narrows the a–b gap from 4.5 mm to 3 mm. Under the higher flux of 60 kW/m²/15 min, wooden-dowel joints reached a = 16.5 mm and b = 11 mm, versus a = 16 mm and b = 11 mm at 60 kW/m²/20 min, demonstrating aggressive surface charring but relatively stable dowel charring. Steel-dowel joints, by contrast, consistently reached a = 17 mm under both 49 kW/m²/20 min and 60 kW/m²/15 min, exceeding wooden configurations by approximately 0.5–2.5 mm. These results confirm that densified wooden dowels moderate heat penetration, maintaining 20–30% lower char depths in the dowel zone, while steel dowels create a pronounced thermal bridge that accelerates surface charring. Increased heat flux and longer durations uniformly deepen char layers across all specimens, but the effect is most pronounced with steel dowels.

Deflection at the free end

Progressive perimeter charring under radiant heating steadily erodes the joint's effective cross-section and flexural rigidity, driving a monotonic increase in free-end deflection. A potentiometer mounted on the top plate continuously tracked this displacement while each L-joint carried a constant vertical load of 51 kg. Figures 11 and 12 document the resulting time-dependent deflection histories for specimens exposed to uniform heat fluxes of 49 kW m^{-2} and 60 kW m^{-2}, respectively. By presenting duplicate tests for both densified-wood and steel dowel configurations, the plots provide a clear basis for assessing how connector material alters the onset, rate, and ultimate magnitude of thermally induced deformation.

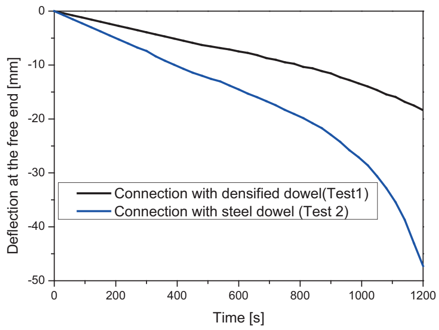

Figure 11. Deflection of the specimen under 49 kW/m² heat flux

Figure 11 records the deflection history of two connections, one assembled with densified-wood dowels and the other with steel dowels, while they are exposed to an external heat flux of 49 kW m^{-2}. Both specimens gradually lose stiffness as charring progresses, but the rate differs markedly: the steel-dowel assembly deflects almost –45 mm after 1,200 s, whereas the densified-dowel counterpart reaches only about –25 mm. The near-linear trajectories in this plot suggest a steady decline in bending stiffness, yet the steeper slope of the steel-dowel curve points to earlier thermal weakening or local slip at the steel-to-wood interface.

Figure 12 reveals that elevating the radiant heat flux to 60 kW m^{-2} magnifies the performance gap between connector types: densified-wood dowel joints level off at roughly –20 to –30 mm of free-end deflection after 900 s, whereas steel-dowel joints plunge far deeper, terminating near –55 mm in Test 1 and almost –100 mm in Test 2—roughly two- to four-times the residual displacement of their wooden counterparts. The divergence emerges within the first 200 s, when both steel-dowel curves steepen sharply, but it is this final displacement gap of up to 70 mm that most clearly underscores the connectors' contrasting fire behaviour: densified dowels appear to stabilise once peripheral charring reaches them, while steel dowels act as thermal bridges that accelerate internal charring and trigger runaway stiffness loss, producing both larger and more scattered ultimate deformations.

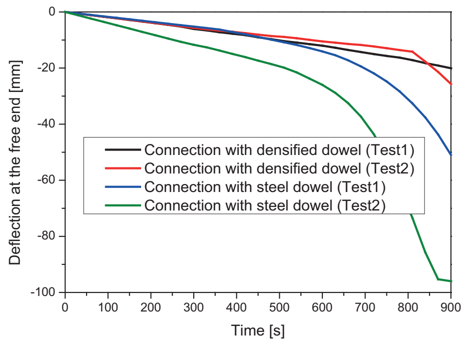

Figure 12. Deflection of the specimen under 60 kW/m² heat flux

Under identical thermal exposures, joints reinforced with thermo-densified wooden dowels consistently outperform those assembled with steel fasteners. At both 49 and 60 kW m^{-2} the wooden-dowel specimens retain flexural stiffness for longer and limit peak free-end deflection to substantially lower values. The contrast is most striking at 60 kW m^{-2}: densified-wood dowels keep the connection in the elastic , whereas steel-dowel joints have already entered inelastic deformation and experience rapid stiffness loss. Replicate tests with wooden dowels also follow nearly identical trajectories, while the steel-dowel tests diverge more noticeably—evidence of the greater predictability and repeatability achieved when metallic heat sinks are eliminated.

From a design perspective, substituting steel dowels with densified wooden dowels can meaningfully delay critical deformation, thereby extending the window for evacuation or active fire-fighting intervention. By avoiding the thermal-bridge effect inherent to steel, wooden dowels reduce peak deflections and enhance the fire resilience and sustainability of mass-timber connections.

CONCLUSION

The experimental programme confirms that replacing conventional steel dowels with thermo-densified wooden dowels markedly enhances the fire performance of engineered-wood connections and CLT panels. At both 49 kW m^{-2} and 60 kW m^{-2} incident heat fluxes, wooden-dowel joints (i) delay the attainment of critical temperatures, (ii) reduce char penetration in the dowel zone by 20–30 %, and (iii) limit free-end deflection to roughly 20–30 mm, compared with 55–100 mm for comparable steel-dowel joints. The advantage is most pronounced at the higher flux: densified-wood dowel joints stay in the elastic while their steel-reinforced counterparts have already entered inelastic deformation and begun to shed stiffness, while the duplicate wooden-dowel tests align far more closely—evidence of tighter repeatability.

Char-pattern analyses reinforce these findings. Unreinforced CLT panels and wooden-dowel joints develop relatively uniform char layers, whereas steel-dowel joints exhibit deep, irregular charring around each connector, evidencing a pronounced thermal-bridge effect that accelerates interior degradation. Measured residual char depths corroborate this behaviour, showing only 0.5–2.5 mm additional char adjacent to densified dowels but substantially deeper local charring around steel fasteners.

From a design perspective, substituting steel dowels with densified wooden dowels can postpone excessive deformation and lengthen the evacuation or intervention window during a fire without introducing metallic heat-sink effects. The results therefore position densified wooden dowels as a sustainable, fire-resilient alternative to metallic fasteners in mass-timber structures. Future work should evaluate long-term durability under hygro-thermal cycling, explore hybrid fastening strategies, and translate these laboratory insights into performance-based design guidelines for adhesive-free engineered-wood construction.

REFERENCES

1. **Fang C.H., Cloutier A., Blanchet P., Koubaa A., Mariotti N.,** Densification of Wood Veneers Combined with Oil-Heat Treatment. Part 1: Dimensional Stability, BioRessources 6 (1), p. 373-385.
2. **Sotayo A., Bradley D., Bather M., Sareh P., Oudjene M., El-Houjeyri I., Harte A.M., Mehra S., O'Ceallaigh C., Haller P., Namari S., Makradi A., Belouettar S., Bouhala L., Deneufbourg F., and Guan Z.** (2020) Review of state of the art of dowel laminated timber members and densified wood materials as sustainable engineered wood products for construction and building applications, Devel. Built Envir. 1, https://doi.org/10.1016/j.dibe.2019.100004.
3. **Anshari B., Guan Z., Kitamori A., Jung K., Hassel I., Komatsu K.,** Mechanical and moisture-dependent swelling properties of compressed Japanese cedar, Construction and Building Materials 25 (2011), p. 1718-1725.
4. **Jung K., Kitamori A., Komatsu K.,** Evaluation on structural performance of compressed wood as shear dowel, Holzforschung 62 (2008), p. 461-467.
5. **Jung K., Kitamori A., Komatsu K.,** Development of a joint system using a compressed wooden fastener I: evaluation of pull-out and rotation performance for a column-sill joint, Journal of Wood Science 55 (2009), p. 273-282.
6. **Jung K., Kitamori A., Komatsu K.,** Development of a joint system using a compressed wooden fastener II: evaluation

of rotation performance for a column-beam joint, Journal of Wood Science 56 (2010a.), p. 118-126.

7. **Jung K., Murakami S., Kitamori A., Chang W.S., Komatsu K.,** Improvement of glued-in-rod joint system using compressed wooden dowel, Holzforschung 64 (2010b), p. 799-804.
8. **Li L., Gong M., Chui Y., Schneider M., Li D.,** Measurement of the elastic parameters of densified balsamfir wood in the radial-tangential plane using a digital image correlation (DIC) method, Journal of Materials Science 48 (2013), p. 7728-7735.
9. **Yoshihara H., Tsunematsu S.,** Bending and shear properties of compressed Sitka spruce, Wood Science and Technology 41 (2007), p. 117-131.
10. **Navi P., Heger F.,** Combined densification and thermo-hydro-mechanical processing of wood, MRS Bull 29 (2004), p. 332-336.
11. **Inoue M., Norimoto M., Tanahashi M., Rowell R.M.,** Steam or heat fixation of compressed wood, Wood and Fiber Science 25 (1993a), p. 224-235.
12. **Song J., Chen C., Zhu S., Zhu M., Dai J., Ray U., Li Y., Kuang Y., Li Y., Quispe N.**, Processing bulk natural wood into a high-performance structural material, Nature 554 (2018) 224.
13. **Bui T.-A, Oudjene M., Khelifa M., Rogaume Y.,** Towards experimental and numerical assessment of the vibrational serviceability comfort of adhesive free laminated timber beams and CLT panels assembled using compressed wood dowels, Eng. Struct. 213C (2020), 110586.
14. **El-Houjeyri I., Thi V.D., Oudjene M., Khelifa M., Sotato A,Guan Z.**, Experimental investigations on adhesive free laminated oak timber beams and timber-to-timber joints assembled using thermo mechanically compressed wood dowels, Constr. Build. Mater. 222 (2019), p. 288–299.
15. **Tran T.T., Thi V.D., Oudjene M., Khelifa M., Girods P., Debal M., Rogaume Y.,** Fire structural performance of thermo-mechanically compressed spruce timber by means experiments and a three-step multi-reactions pyrolysis 3D-finite element modelling, Constr. Build. Mater. 320 (2022).
16. ISO 834-1, Fire resistance tests-Elements of building construction-Part 1: General requirements, International Organization for Standardization, 1999.
17. EN 1995-1-1:2004, Eurocode 5: design of timber structures – part 1. 1: general rules and rules for buildings, European Committee for Standardization, Brussels, Belgium, (E).

СПИСОК ЛИТЕРАТУРЫ

1. **Fang C.H., Cloutier A., Blanchet P., Koubaa A., Mariotti N.** Densification of Wood Veneers Combined with Oil-Heat Treatment. Part 1: Dimensional Stability, BioRessources 6 (1), p. 373-385.
2. **Sotayo A., Bradley D., Bather M., Sareh P., Oudjene M., El-Houjeyri I., Harte A.M., Mehra S., O'Ceallaigh C., Haller P., Namari S., Makradi A., Belouettar S., Bouhala L., Deneufbourg F., and Guan Z.** (2020) Review of state of the art of dowel laminated timber members and densified wood materials as sustainable engineered wood products for construction and building applications, Devel. Built Envir. 1, https://doi.org/10.1016/j.dibe.2019.100004.
3. **Anshari B., Guan Z., Kitamori A., Jung K., Hassel I., Komatsu K**. Mechanical and moisture-dependent swelling properties of compressed Japanese cedar, Construction and Building Materials 25 (2011), p. 1718-1725.
4. **Jung K., Kitamori A., Komatsu K**., Evaluation on structural performance of compressed wood as shear dowel, Holzforschung 62 (2008), p. 461-467.
5. **Jung K., Kitamori A., Komatsu K.,** Development of a joint system using a compressed wooden fastener I: evaluation of pull-out and rotation performance for a column-sill joint, Journal of Wood Science 55 (2009), p. 273-282.

6. **Jung K., Kitamori A., Komatsu K.,** Development of a joint system using a compressed wooden fastener II: evaluation of rotation performance for a column-beam joint, Journal of Wood Science 56 (2010a.), p. 118-126.
7. **Jung K., Murakami S., Kitamori A., Chang W.S., Komatsu K.,** Improvement of glued-in-rod joint system using compressed wooden dowel, Holzforschung 64 (2010b), p. 799-804.
8. **Li L., Gong M., Chui Y., Schneider M., Li D.,** Measurement of the elastic parameters of densified balsamfir wood in the radial-tangential plane using a digital image correlation (DIC) method, Journal of Materials Science 48 (2013), p. 7728-7735.
9. **Yoshihara H., Tsunematsu S.,** Bending and shear properties of compressed Sitka spruce, Wood Science and Technology 41 (2007), p. 117-131.
10. **Navi P., Heger F.,** Combined densification and thermo-hydro-mechanical processing of wood, MRS Bull 29 (2004), p. 332-336.
11. **Inoue M., Norimoto M., Tanahashi M., Rowell R.M.,** Steam or heat fixation of compressed wood, Wood and Fiber Science 25 (1993a), p. 224-235.
12. **Song J., Chen C., Zhu S., Zhu M., Dai J., Ray U., Li Y., Kuang Y., Li Y., Quispe N.**, Processing bulk natural wood into a high-performance structural material, Nature 554 (2018) 224.
13. **Bui T.-A, Oudjene M., Khelifa M., Rogaume Y.,** Towards experimental and numerical assessment of the vibrational serviceability comfort of adhesive free laminated timber beams and CLT panels assembled using compressed wood dowels, Eng. Struct. 213C (2020), 110586.
14. **El-Houjeyri I., Thi V.D., Oudjene M., Khelifa M., Sotato A,Guan Z.**, Experimental investigations on adhesive free laminated oak timber beams and timber-to-timber joints assembled using thermo mechanically compressed wood dowels, Constr. Build. Mater. 222 (2019), p. 288–299.
15. **Tran T.T., Thi V.D., Oudjene M., Khelifa M., Girods P., Debal M., Rogaume Y.,** Fire structural performance of thermo-mechanically compressed spruce timber by means experiments and a three-step multi-reactions pyrolysis 3D-finite element modelling, Constr. Build. Mater. 320 (2022).
16. ISO 834-1, Fire resistance tests-Elements of building construction-Part 1: General requirements, International Organization for Standardization, 1999.
17. EN 1995-1-1:2004, Eurocode 5: design of timber structures – part 1. 1: general rules and rules for buildings, European Committee for Standardization, Brussels, Belgium, (E).

T.T. Tran – Hanoi Architectural University, Km 10, Nguyen Trai street, Thanh Xuan district, Hanoi city, VIETNAM , e-mail: tuantt@hau.edu.vn

M. Khelifa – University of Lorraine, Lermab, EA 4370, 27 rue Philippe Seguin, 88051 Epinal, France, e-mail: tuantt@hau.edu.vn

M. Oudjene – Department of Civil and Water Engineering, University of Laval, 1065 avenue de la Médecine, Québec, Canada, e-mail: tuantt@hau.edu.vn

M. Debal – University of Lorraine, Lermab, EA 4370, 27 rue Philippe Seguin, 88051 Epinal, France, e-mail: tuantt@hau.edu.vn

Y. Rogaume – University of Lorraine, Lermab, EA 4370, 27 rue Philippe SEGUIN, 88051 Epinal, France, e-mail: tuantt@hau.edu.vn

Т.Т. Тран – Ханойский архитектурный университет, 10, улица Нгуен Траи, район Тхань Суан, город Ханой, Вьетнам, e-mail: tuantt@hau.edu.vn

М. Хелифа – Университет Лотарингии, ЛЕРМАБ, EA 4370, 27 улица Филиппа Сегуина, 88051 Эпинал, ФРАНЦИЯ, e-mail: tuantt@hau.edu.vn

М. Уджене – Факультет гражданского и водного строительства, Университет Лаваля, 1065 проспект Медицины, Квебек, Канада, e-mail: tuantt@hau.edu.vn

М. Дебал – Университет Лотарингии, ЛЕРМАБ, EA 4370, 27 улица Филиппа Сегуина, 88051 Эпинал, Франция, e-mail: tuantt@hau.edu.vn

Ю. Рогаум – Университет Лотарингии, ЛЕРМАБ, EA 4370, 27 улица Филиппа Сегуина, 88051 Эпинал, Франция, e-mail: tuantt@hau.edu.vn